Optical investigations of chemically pressurized $EuFe_2(As_{1-x}P_x)_2$: An *s*-wave superconductor with strong interband interactions

D. Wu,[1] G. Chanda,[1] H. S. Jeevan,[2] P. Gegenwart,[2] and M. Dressel[1]

[1]*Physikalisches Institut, Universität Stuttgart, Pfaffenwaldring 57, DE-70550 Stuttgart, Germany*
[2]*Physikalisches Institut, Georg-August-Universität Göttingen, DE-37077 Göttingen, Germany*

Superconducting $EuFe_2(As_{0.82}P_{0.18})_2$ single crystals are investigated by broad-band infrared spectroscopy. Below $T_c = 28$ K, a superconducting gap forms at $2\Delta_0 = 9.5$ meV $= 3.7k_BT_c$, causing the reflectivity to sharply rise to unity at low frequency. In the range of the gap, the optical conductivity can be perfectly described by BCS theory with an *s*-wave gap and no nodes. From our analysis of the temperature-dependent conductivity and spectral weight at $T > T_c$, we deduce an increased *interband* coupling between hole and electron sheets on the Fermi surface when T approaches T_c.

From the intense study of iron pnictides over the last years, two main facts became clear. (1) Optimum superconductivity is reached when long-range magnetic order and structural transition are completely suppressed by doping or pressure; magnetic excitations are superior constituents to superconductivity. (2) Multiband models are needed to describe the low-energy electronic excitations in pnictides and to account for the complexity and interplay of magnetic and superconducting orders; both intraband and interband interactions play important roles.[1,2] To clarify the possible mechanisms, it is important to investigate the electrodynamics of charge carriers in compounds with altered Fermi-surface environment.

The isovalent-substituted $MFe_2(As_{1-x}P_x)_2$ system ($M =$ Ba, Eu, Sr) is an ideal candidate for this purpose because the chemical-pressure-induced superconductivity has a transition temperature as high as obtained by carrier doping.[3,4] Band structure calculations show that P substitution significantly changes the shape of the hole sheets at Γ point and, finally, one of the three hole sheets is absent in $BaFe_2P_2$.[5,6] Carrier doping (for example, hole-doped $Ba_{1-x}K_xFe_2As_2$), on the other hand, mainly affects the size of the sheets, although it influences the Fermi-surface (FS) reconstruction as well.[7–9] The isovalent substitution of As by P keeps the balance between the electron and hole numbers and avoids possible scattering effects by charged impurities within the Fe-As planes, which is still ambiguous in carrier-doped systems.

Here we present an optical study on $EuFe_2(As_{0.82}P_{0.18})_2$ in wide temperature and energy ranges. When crossing T_c, clear evidence of a superconducting gap is observed at 74 cm^{-1}. The normalized conductivity resembles the BCS behavior with a complete gap $2\Delta_0 = 3.7k_BT_c$ without nodes. In the normal state, upon cooling, the spectral weight of the Drude component partially moves to a mid-infrared incoherent contribution, which is referred to as effect of spin-fluctuation-induced interband interaction.

Single crystalline samples of $EuFe_2(As_{0.82}P_{0.18})_2$ were grown as described in Ref. 10. Specific heat and magnetic susceptibility measurements indicate a bulk superconducting transition at 28 K, followed by the magnetic ordering of Eu^{2+} moments at 18 K.[11] The temperature-dependent reflectivity spectra were measured in a wide frequency range from 20 to 37 000 cm^{-1} using two Fourier-transform infrared spectrometers (30–15 000 cm^{-1}) and a variable-angle spectroscopic ellipsometer extending up to the ultraviolet (6000–37 000 cm^{-1}, restricted to room temperature). Setups with two different 1.6 K bolometers (10–60 and 20–100 cm^{-1}) have been employed to check and independently confirm the low-frequency reflectivity around the superconducting gap (below 100 cm^{-1}).

In Fig. 1(b), we show the in-plane reflectivity $R(\omega)$ of $EuFe_2(As_{0.82}P_{0.18})_2$ at selected temperatures; panel 1(a) is a blowup of the low-frequency part. The reflectivity has a metallic behavior both in frequency and temperature. Below T_c, an upturn with a change of curvature appears in $R(\omega)$ at around 100 cm^{-1}; at the lowest temperature, the reflectivity reaches unity at 74 cm^{-1}. This is strong evidence for the superconducting gap formation. The real part of the optical conductivity $\sigma_1(\omega,T)$ calculated through Kramers-Kronig procedure is shown in panels 1(c) and 1(e) for different spectral ranges. Up to 4000 cm^{-1}, $\sigma_1(\omega, T > T_c)$ can be well described by a narrow Drude contribution σ_N ($\tau_{30\,K}^{-1} \approx 30$ cm^{-1}, $\omega_p = 5730$ cm^{-1}) plus a flat plateau, which previously has been defined as a "broad Drude" σ_B ($\tau_{30\,K}^{-1} \approx 440$ cm^{-1}, $\omega_p = 6800$ cm^{-1}), in addition to a Lorentzian component center at $\omega_0 = 970$ cm^{-1}.[12–15] For $T < T_c$, $\sigma_1(\omega)$ drops rapidly to zero with decreasing frequency, indicating a nodeless *s*-wave superconducting gap. $\sigma_1(\omega)$ at higher energies can be modeled by several Lorentzian-type contributions, as demonstrated in Fig. 1(d).

Multiple superconducting gaps have been reported in the literature for the 122-family of pnictides,[16] which is not surprising for multiband materials.[2] With this in mind, we also performed a BCS-based gap analysis for the optical properties of $EuFe_2(As_{0.82}P_{0.18})_2$ to see whether we gain information on the number of gaps and their magnitude. As mentioned above, two superimposed Drude components σ_N and σ_B are needed to describe the normal state conductivity of $EuFe_2(As_{0.82}P_{0.18})_2$. Correspondingly, we tried to decompose the conductivity in the superconducting state $\sigma^{(s)}$ as $\sigma_N^{(s)} + \sigma_B^{(s)}$ assuming no interplay between them. In the simplest case, each of these independent components is described by the BCS theory[17] in the form given in Ref. 18. Surprisingly, the best description of $\sigma^{(s)}/\sigma^{(n)}$ is reached using the same gap parameter:
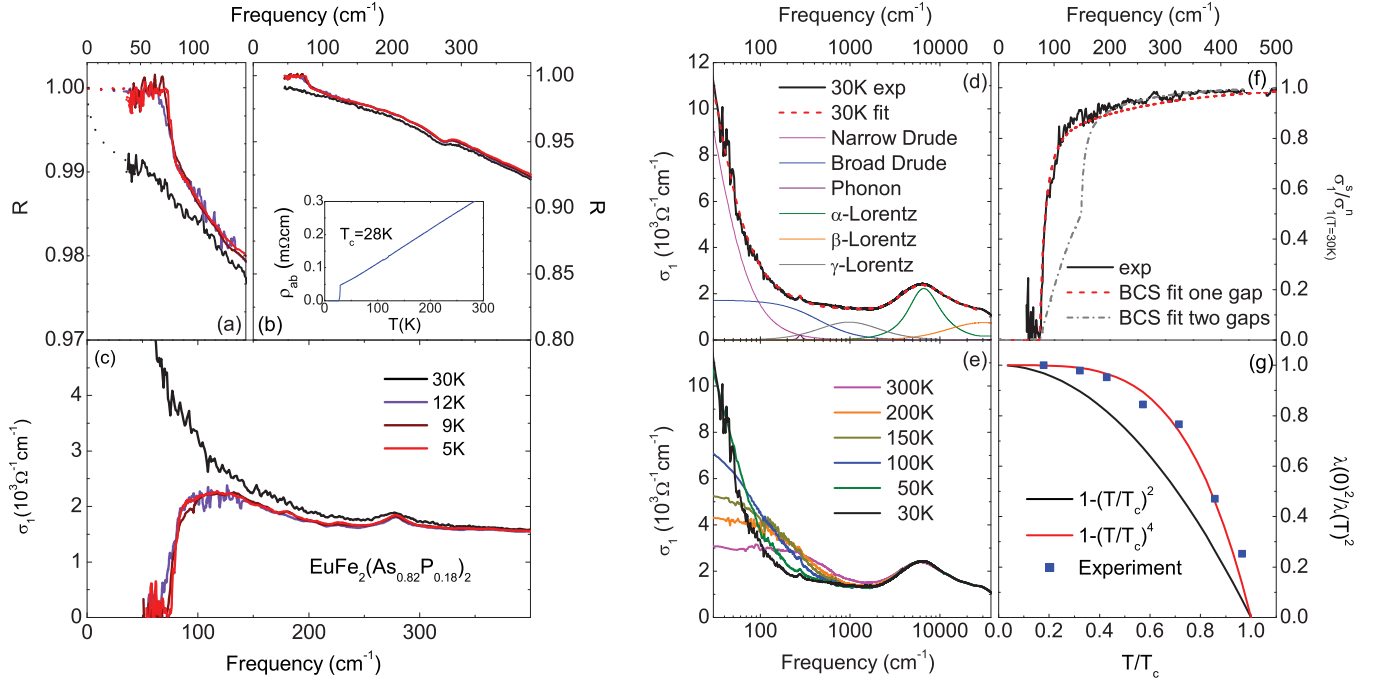
FIG. 1. (Color online) Optical properties of $EuFe_2(As_{0.82}P_{0.18})_2$ in the ab plane measured in a broad frequency range at different temperatures. (a), (b) The reflectivity $R(\omega)$ increases with a change of curvature around 100 cm^{-1} for $T < 28$ K and approaches unity at 74 cm^{-1}, which is a signature for a superconducting gap formation. Inset: in-plane dc resistivity. The superconducting transition occurs at $T = 28$ K, where $\rho(T)$ sharply decreases to zero. (c) Below 28 K, the sudden drop of $\sigma_1(\omega)$ to zero indicates a nodeless s-wave superconducting gap. (d) Drude-Lorentz fit for the normal-state conductivity ($T = 30$ K). (e) In the normal state, $\sigma_1(\omega)$ develops as a metal upon cooling. (f) Ratio of $\sigma_1(\omega)$ in the normal ($T = 30$ K) and superconducting states $\sigma_1^{(s)}(\omega)/\sigma_1^{(n)}(\omega)$ of $EuFe_2(As_{0.82}P_{0.18})_2$ at $T = 5$ K. The dashed red line corresponds to the fit by the BCS model using a single gap of $2\Delta_0 = 74$ cm^{-1}, while the dashed gray line refers to the two-gap scenario with $2\Delta_N = 150$ cm^{-1} and $2\Delta_B = 74$ cm^{-1}. (g) Penetration depth as a function of temperature plotted in a renormalized fashion. The experimental data of $EuFe_2(As_{0.82}P_{0.18})_2$ can be described with $1 - (T/T_c)^4$.

$2\Delta_N = 2\Delta_B = 74$ cm^{-1}, as shown in Fig. 1(f). This implies a single s-wave gap $2\Delta_0 = 3.7k_BT_c$ in $EuFe_2(As_{0.82}P_{0.18})_2$. Note that, with $2\Delta_N > \tau_N^{-1}$, the narrow Drude falls into the clean limit, where a gap is difficult be be observed in σ_1. Nevertheless, our calculations of $\sigma_1(\omega)$ evidence that assuming a second larger gap $2\Delta_N = 150$ cm^{-1} ($\sim7.7k_BT_c$, a typical value for large gap in pnictides) would cause a clear drop of σ_1 of about 600 $(\Omega\,$cm$)^{-1}$ at 150 cm^{-1}—a similar effect can be also seen from $\sigma_1^{(s)}(\omega)/\sigma_1^{(n)}(\omega)$, as shown in Fig. 1(f). Since we do not observe any of this kind of decrease in our measured data from 75–400 cm^{-1}, we conclude the absence of a second larger gap in $EuFe_2(As_{0.82}P_{0.18})_2$. Furthermore, it is not necessary to introduce nodes in the gap, as recently suggested[19,20] from experiments on $BaFe_2(As_{1-x}P_x)_2$. Although there is a low-energy limit of our optical data, at that point the reflectance is flat and close to unity, leaving no space for nodes below the measurement frequencies. This issue can be due to magnetic scattering induced by Eu^{2+} ions that may lift the nodes. Further investigation is needed to support this suggestion.

From the optical conductivity, we extract the superconducting penetration depth $\lambda(T)$ of $EuFe_2(As_{0.82}P_{0.18})_2$. According to the Ferrell-Glover-Tinkham sum rule,[17] the missing spectral weight $A = \int_{0+}^{\infty}[\sigma_1^{(n)}(\omega) - \sigma_1^{(s)}(\omega)]d\omega$ is connected to the superfluid density $\rho_s = 8A/c^2$ and to the penetration depth as $A = c^2/8\lambda^2$. Alternatively, one can also estimate $\lambda(T)$ from the imaginary part of the complex conductivity in

the low-frequency limit: $\sigma_2(\omega) = \frac{\pi N_s e^2}{m\omega} = \frac{c^2}{4\pi\lambda^2\omega}$. We consistently obtain $\lambda(T \to 0) \approx 300$ nm, which is very close to the value found for the other 122 iron pnictides, such as $Ba(Fe_{0.92}Co_{0.08})_2As_2$ and $Ba(Fe_{0.95}Ni_{0.05})_2As_2$.[14] The temperature dependence of the penetration depth is plotted in Fig. 1(g) in the form of $\lambda(0)^2/\lambda(T)^2$ versus T/T_c. The data fall nicely onto the curve $1 - (T/T_c)^4$ as predicted by the two-fluid model and commonly used to describe a simple s-wave gap at moderate T. These findings are consistent with our gap analysis and confirm the s-wave superconducting gap formation in $EuFe_2(As_{0.82}P_{0.18})_2$.

Above, we concluded that a large superconducting gap ($2\Delta_0 \gg 3.5k_BT_c$) is absent in this P-substituted MFe_2As_2 material, albeit in the carrier-doped iron pnictides multiple gaps with large values are commonly found.[16,21–24] To understand this difference, we have to consider the band structure, as depicted in Fig. 2. The undoped MFe_2As_2 contains three sheets of Fermi surface with hole character (h-FS) at the Γ point and two electron sheets (e-FS) at the M point of the Brillouin zone.[6,9,25] While the inner two h-FSs and the two e-FSs are basically two dimensional, the third h-FS is more three dimensional, as it has a stronger dispersion along k_z.[26] The antiferromagnetic (spin-density-wave) ordering happens along the nesting vector Q_n indicated by the arrow. With hole doping, the h-FSs and e-FSs expand and shrink, respectively, along the k_xk_y plane [Fig. 2(b)], causing a considerable
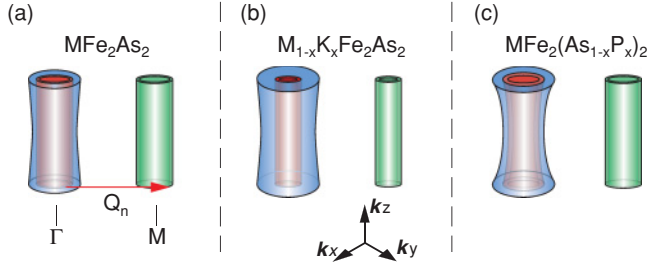
FIG. 2. (Color online) Fermi sheets in first Brillouin zone for $M\text{Fe}_2\text{As}_2$ family (M = Ba, Eu, Sr). Three sheets at the Γ point are holelike Fermi surfaces, and two at the M point are electronlike Fermi surfaces. (a) Parent compound $M\text{Fe}_2\text{As}_2$; (b) hole doping leads to a change in the diameter of the Fermi surface in $M_{1-x}\text{K}_x\text{Fe}_2\text{As}_2$. The large gap $2\Delta_0 = 7.5k_BT_c$ opens at the inner two hole-FSs (red sheets) and two electron-FSs (green sheets), while the small gap $2\Delta_0 = 3.7k_BT_c$ opens at the outer hole-FS (blue sheet). (c) P substitution in $M\text{Fe}_2(\text{As}_{1-x}\text{P}_x)_2$ changes the warping of the Fermi surface and thus reduces the two-dimensional character.

weakening of the nesting; spin fluctuations increase. Angle-resolved photoemission spectroscopy (ARPES) studies on optimally doped $\text{Ba}_{0.6}\text{K}_{0.4}\text{Fe}_2\text{As}_2$ show that the dispersion of the FSs remains similar to the undoped compounds; a large portion of the inner h-FSs is still connected (quasinested) to the e-FSs by the same Q_n, and this enhances the scattering from the e-FSs to the h-FSs and yields a very large pairing strength ($2\Delta_0 = 7.5k_BT_c$) for these FSs.[7]

In P-substituted $M\text{Fe}_2\text{As}_2$, on the contrary, the isovalent substitution does not introduce carriers, hence no expansion or shrinkage of FSs is expected. However, according to band structure calculations,[5,6,27] the P substitution can enhance the dimensionality of h-FSs since it is very sensitive to the pnictogen position. As observed in recent ARPES investigations on P-substituted $\text{EuFe}_2(\text{As}_{1-x}\text{P}_x)_2$, the k_z dispersion increases and varies along the Γ-Z line while it remains small and is slightly modified along the K-X line, namely, the h-FSs start to warp but e-FSs keep almost unchanged upon P substitution.[28] Such warpings of hole-FSs break the nesting condition and eventually enable superconductivity. At the same time, the three warped h-FSs rule out the possibility for their large geometric overlapping with two e-FSs, which would cause a large pairing strength as discussed above for carrier-doped pnictides. This peculiarity of the P-substituted systems can explain the absence of a *large* superconducting gap in $\text{EuFe}_2(\text{As}_{0.82}\text{P}_{0.18})_2$. Interestingly, although the "quasinesting" between the FSs in the P-substituted case is not as good as the one with carrier doping, the pairing constant we observed here is not getting much lower either ($2\Delta_0 = 3.7k_BT_c$); it is still comparable with the smaller gap found in, for example, $\text{Ba}_{0.6}\text{K}_{0.4}\text{Fe}_2\text{As}_2$ where $2\Delta_0 = 3.8k_BT_c$. Considering this issue together with the very similar critical temperatures of $\text{EuFe}_2(\text{As}_{0.82}\text{P}_{0.18})_2$ and $\text{Ba}_{0.6}\text{K}_{0.4}\text{Fe}_2\text{As}_2$, one could suspect that the three-dimensional character of the h-FS(s) is one of the obstacles to raise a higher T_c in pnictide.

More insight into the *interband* interaction between hole and electron bands is obtained from our spectral weight analysis, in particular, when we consider a spectral weight redistribution from low to high energies upon cooling.
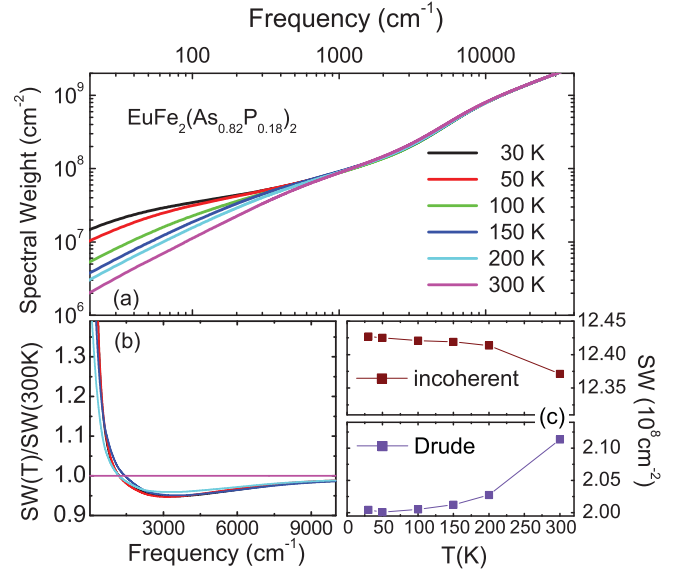

FIG. 3. (Color online) (a) The spectral weight $\text{SW}(\omega_c) = 8\int_0^{\omega_c} \sigma_1(\omega)\,d\omega$ as a function of cutoff frequency ω_c for several temperatures. (b) The normalized spectral weight $\text{SW}(T)/\text{SW}$ (300 K). A minimum can be found at $\omega_{\min} \approx 3000$ cm^{-1}. (c) The spectral weight for the mid-infrared component α-Lorentz and the Drude component plotted as a function of temperature for $T > T_c$.

In Fig. 3(a), the spectral weight $\text{SW}(\omega_c) = 8\int_0^{\omega_c} \sigma_1(\omega)\,d\omega$ is plotted as a function of cutoff frequency ω_c. Up to 10 000 cm^{-1}, the $\text{SW}(\omega_c,T)$ is still not conserved. An upturn around 3000–5000 cm^{-1} is observed, indicating that a spectral weight redistribution starts within this frequency range. To elucidate this point, we normalize $\text{SW}(T < 300\text{ K})$ to $\text{SW}(300\text{ K})$ and plot it in Fig. 3(b). We find that the spectral weight is reduced up to 5%, an effect beyond the uncertainty of experiments. We also notice that, below the $\omega_{\min}$ (defined as a frequency where the relative spectral weight reaches its minimum), the normalized SW drops faster upon cooling as typical for a Drude behavior that narrows with decreasing temperature. Above $\omega_{\min}$, the ratio $\text{SW}(T < 300)$ to $\text{SW}(300\text{ K})$ increases as the incoherent process starts to dominate the spectral weight. We can easily extract the Drude and incoherent component by taking $\text{SW}_{\text{Drude}} = \text{SW}(\omega_{\min})$ and $\text{SW}_{\text{incoherent}} = \text{SW}_{\text{cons}} - \text{SW}(\omega_{\min})$, as plotted in Fig. 3(c); here SW_{cons} is the spectral weight approached for large frequencies, in practice, $\omega \approx 10\,000$ cm^{-1}. With decreasing temperature, SW_{Drude} is continuously reduced and the lost SW piles up at the incoherent contribution. Normally, the reduction of the Drude-part spectral weight can be associated to mass enhancement of carriers induced by Fermi-surface shrinkage.[29,30] But the FS shrinking in a single band model (or, in other words, a model without involving many-body interaction effects) is usually rigid-band-shift-like and it will not cause an additional transfer of spectral weight to the incoherent processes. In pnictides, the carriers interact via a bosonic mode, while the largest source of interactions comes from the exchange of spin fluctuations between quasinested hole and electron pockets, indicating a predominant *interband* character of the interactions.[1,2,30] Such an *interband* interaction, together with the Coulomb repulsion which occurs at higher energy, can induce a FS shrinking with

a very different redistribution of the spectral weight in the density of states (DOS) from the one in the rigid band shift.[30] As described by Benfatto and Cappelluti, the peculiar long tail in the DOS can be considered as a characteristic signature of the interband nature of interaction. More important in the context of optical properties, it causes an enhanced incoherent contribution aside from the reduction of coherent Drude part. Since this is consistent with our present findings, we consider the observed spectral weight transfer from the Drude to incoherent contributions in optics as experimental evidence for the spin-fluctuation-induced *interband* interaction. The continuous transfer of spectral weight upon cooling, namely, a stronger interband-interaction-induced FS shrinkage with decreasing temperature, should then imply stronger spin fluctuations as T_c is approached.

Our infrared study on isovalent P-substituted EuFe$_2$(As$_{0.82}$P$_{0.18}$)$_2$ gives clear evidence for the formation of a single nodeless *s*-wave superconducting gap. From the comparison with the multigap scenario of carrier-doped iron pnictides, we found that the similarity in geometry and dimension between hole and electron Fermi-surface sheets has a strong influence not only on the nesting for the spin-density-wave state but also on the pairing conditions for the superconducting state. This is considered as another indication that the pairing between the Fermi surface sheets very much relies on spin excitations along the nesting vector; in other words, superconductivity in iron pnictide has magnetic origin. The continuous spectral weight transfer upon cooling from the coherent (Drude) to the incoherent contributions indicates an enhanced spin-fluctuation-induced interband interaction as the superconducting transition is approached.

[1] I. I. Mazin, Nature (London) **464**, 183 (2010).

[2] D. C. Johnston, Adv. Phys. **59**, 803 (2010).

[3] Z. Ren, Q. Tao, S. Jiang, C. M. Feng, C. Wang, J. H. Dai, G. H. Cao, and Z.-A. Xu, Phys. Rev. Lett. **102**, 137002 (2009).

[4] S. Jiang, H. Xing, G. F. Xuan, C. Wang, Z. Ren, C. M. Feng, J. H. Dai, Z-A. Xu, and G. H. Cao, J. Phys. Condens. Matter **21**, 382203 (2009).

[5] H. Shishido, A. F. Bangura, A. I. Coldea, S. Tonegawa, K. Hashimoto, S. Kasahara, P. M. C. Rourke, H. Ikeda, T. Terashima, R. Settai, Y. Ōnuki, D. Vignolles, C. Proust, B. Vignolle, A. McCollam, Y. Matsuda, T. Shibauchi, and A. Carrington, Phys. Rev. Lett. **104**, 057008 (2010).

[6] S. Kasahara, T. Shibauchi, K. Hashimoto, K. Ikada, S. Tonegawa, R. Okazaki, H. Shishido, H. Ikeda, H. Takeya, K. Hirata, T. Terashima, and Y. Matsuda, Phys. Rev. B **81**, 184519 (2010).

[7] H. Ding, P. Richard, K. Nakayama, K. Sugawara, T. Arakane, Y. Sekiba, A. Takayama, S. Souma, T. Sato, T. Takahashi, Z. Wang, X. Dai, Z. Fang, G. F. Chen, J. L. Luo, and N. L. Wang, Europhys. Lett. **83**, 47001 (2008).

[8] K. Terashima, Y. Sekiba, J. H. Bowen, K. Nakayama, T. Kawahara, T. Sato, P. Richard, Y.-M. Xu, L. J. Li, G. H. Cao, Z.-A. Xu, H. Ding, and T. Takahashi, Proc. Natl. Acad. Sci. USA **106**, 7330 (2009).

[9] J. Paglione and R. L. Greene, Nat. Phys. **6**, 645 (2010).

[10] H. S. Jeevan, Z. Hossain, D. Kasinathan, H. Rosner, C. Geibel, and P. Gegenwart, Phys. Rev. B **78**, 092406 (2008); **78**, 052502 (2008).

[11] H. S. Jeevan, D. Kasinathan, H. Rosner, and P. Gegenwart, e-print arXiv:1011.4481.

[12] J. J. Tu, J. Li, W. Liu, A. Punnoose, Y. Gong, Y. H. Ren, L. J. Li, G. H. Cao, Z. A. Xu, and C. C. Homes, Phys. Rev. B **82**, 174509 (2010)

[13] E. G. Maksimov, A. E. Karakozov, B. P. Gorshunov, V. S. Nozdrin, A. A. Voronkov, E. S. Zhukova, S. S. Zhukov, Dan Wu, M. Dressel, S. Haindl, K. Iida, and B. Holzapfel, e-print arXiv:1008.3473.

[14] D. Wu, N. Barisic, P. Kallina, A. Faridian, B. Gorshunov, N. Drichko, L. J. Li, X. Lin, G. H. Cao, Z. A. Xu, N. L. Wang, and M. Dressel, Phys. Rev. B **81**, 100512(R) (2010).

[15] N. Barisic, D. Wu, M. Dressel, L. J. Li, G. H. Cao, and Z.-A. Xu, Phys. Rev. B **82**, 054518 (2010).

[16] M. Dressel, D. Wu, N. Barišić, and B. Gorshunov, J. Phys. Chem. Solids, doi:10.1016/j.jpcs.2010.10.004 (in press, 2010), and references therein.

[17] M. Dressel and G. Grüner, *Electrodynamics of Solids* (Cambridge University Press, Cambridge, 2002).

[18] W. Zimmermann, E. H. Brandt, M. Bauer, E. Seider, and L. Genzel, Phys. C (Amsterdam) **183**, 99 (1991).

[19] K. Hashimoto, M. Yamashita, S. Kasahara, Y. Senshu, N. Nakata, S. Tonegawa, K. Ikada, A. Serafin, A. Carrington, T. Terashima, H. Ikeda, T. Shibauchi, and Y. Matsuda, Phys. Rev. B **81**, 220501 (2010).

[20] Y. Nakai, T. Iye, S. Kitagawa, K. Ishida, S. Kasahara, T. Shibauchi, Y. Matsuda, and T. Terashima, Phys. Rev. B **81**, 020503 (2010).

[21] G. Li, W. Z. Hu, J. Dong, Z. Li, P. Zheng, G. F. Chen, J. L. Luo, and N. L. Wang, Phys. Rev. Lett. **101**, 107004 (2008).

[22] D. Wu, N. Barišić, M. Dressel, G. H. Cao, Z. A. Xu, J. P. Carbotte, and E. Schachinger, Phys. Rev. B **82**, 184527 (2010).

[23] K. W. Kim, M. Rössle, A. Dubroka, V. K. Malik, T. Wolf, and C. Bernhard, Phys. Rev. B **81**, 214508 (2010).

[24] E. van Heumen, Y. Huang, S. de Jong, A. B. Kuzmenko, M. S. Golden, and D. van der Marel, Europhys. Lett. **90**, 37005 (2010).

[25] L. Zhang and D. J. Singh, Phys. Rev. B **79**, 174530 (2009).

[26] G. T. Wang, Y. M. Qian, G. Xu, X. Dai, and Z. Fang, Phys. Rev. Lett. **104**, 047002 (2010).

[27] J. G. Analytis, C. M. J. Andrew, A. I. Coldea, A. McCollam, J.-H. Chu, R. D. McDonald, I. R. Fisher, and A. Carrington, Phys. Rev. Lett. **103**, 076401 (2009).

[28] S. Thirupathaiah, E. D. L. Rienks, H. S. Jeevan, R. Ovsyannikov, E. Slooten, J. Kaas, E. van Heumen, S. de Jong, H. A. Duerr, K. Siemensmeyer, R. Follath, P. Gegenwart, M. S. Golden, and J. Fink, e-print arXiv:1007.5205.

[29] L. Ortenzi, E. Cappelluti, L. Benfatto, and L. Pietronero, Phys. Rev. Lett. **103**, 046404 (2009).

[30] L. Benfatto and E. Cappelluti, e-print arXiv:1011.5397.